

Microbial Competition in Reactors with Wall Attachment: A Comparison of Chemostat and Plug Flow Models

Mary M. Ballyk, Don A. Jones, and Hal L. Smith
Department of Mathematics
Arizona State University
Tempe, AZ 85287-1804

January 26, 1999

1 Introduction

The indigenous microflora of the human large intestine is a complex ecosystem consisting of several hundred species of microorganisms [5]. The composition of the microflora is remarkably stable; the species coexist without one or a few becoming dominant [12]. One of its most important contributions to the host is its ability to impede the colonization of the intestinal tract by nonindigenous microorganisms [19]. The term “colonization resistance” [22] is used to describe all mechanisms involved in this function. An understanding of these mechanisms would represent a major contribution to human health. Competition for nutrients and competition for adhesion sites appear to be widely accepted as among the most important components of colonization resistance [4, 12, 13, 14, 19, 20].

The difficulties associated with *in vivo* studies of the human intestinal microflora are self-evident. A number of *in vitro* models of bacterial interactions in the gut have been proposed by various authors. Rolfe [19] states that the chemostat, or continuous-stirred tank reactor (CSTR), is likely the best system for the study of bacterial interactions, since complex population levels of several different organisms can be maintained. Freter and his

co-workers [6, 7, 8, 9, 10, 11] use the CSTR as an *in vitro* model of the mouse large intestine. Hume [12] suggests that, when examining digestive processes, this region of the vertebrate gut is best modeled by a modified plug flow reactor, which consists of a number of stirred tanks connected in series. Macfarlane et. al. [15] use a three-vessel modified plug flow reactor as an *in vitro* model of the physiology and ecology of microorganisms in the human colon. Penry and Jumars [18] assert that as the number of stirred tanks increases, this reactor system becomes more and more like the plug flow reactor (PFR). In this paper we focus on the performance of the PFR as a model of the human large intestine from an ecological standpoint.

In a series of papers [6, 7, 8, 9, 10, 11] Freter and his co-workers examine, both experimentally and mathematically, the observed stability of an indigenous intestinal microflora. Two-strain models of the gut, with the CSTR as their basis and incorporating wall growth, are formulated and numerically investigated in [6, 10]. In [6] an invading strain is introduced at the steady state of an already established (resident) strain. Numerical simulations indicate that the invader is virtually eliminated, despite the fact it is identical to the resident in all respects. In [10], the mathematical model of [6] is reformulated to investigate the role of adhesion in the implantation of an invading strain. It is found that a less competitive invader can establish and coexist with the resident provided it has specific sites available for adhesion.

Motivated by Freter's work on the gut, the authors formulated a very general model of multi-strain competition for limiting nutrient and for limited adhesion sites in [1]. The single-strain case of the general model is analyzed in [2]. Instead of the CSTR as in Freter's work, the model is based on the PFR. Penry and Jumars [18] argue that the plug flow model is more appropriate for the human gut (and most other mammals). Substrate concentrations in the PFR are maintained at higher levels at the inlet and decline along the length of the reactor. In contrast, the concentration of substrate in the CSTR is diluted immediately upon entering the growth vessel. The PFR model also allows for spatial heterogeneity and material flow, neither of which can be considered in the CSTR. However, we have found that rapid nutrient diffusion and microbial motility in the PFR model accurately approximate the continuous-stir hypothesis of the CSTR model. The result is a remarkable correspondence with the numerical results of Freter et. al. [6, 10]. This correspondence is explored in section 2.

In section 3 we present a numerical investigation of the performance of the PFR model in a biologically reasonable context. Reactor dimensions (length,

radius) are chosen in accordance with data on the large intestine, while the velocity of the medium is varied to reflect realistic transit times. Additionally, the PFR model allows for the consideration of the effect of nutrient diffusion and random cell motility on bacterial interactions in the gut. Such behaviors are not considered in the CSTR models of Freter et. al. [6, 10]. Finally, nutrient uptake functions, rates of adhesion and shedding, and the nutrient input concentration are as in Freter et. al. [6, 10], so that comparisons can be made with the simulations of section 2. *I have not yet included a synopsis of the results of section 3 here.*

I have not yet mentioned the segregation effect. There is a nice quote in Hume [12], p.95, that might be of some use. He says, "From these general principles it would be predicted that the bacterial population adhering to the epithelium would be even more stable than that in the lumen. In this case the invader must compete with the resident species or strains not only for limiting nutrients but also for specific adhesion sites. Indeed, the bacteria adhering to the gut wall appear to be not only very stable in species composition but very specialized as well, forming dense mats of often virtually pure cultures. This specificity in adhesion sites may not only be physical but also an effect of local immune reactions of the hundgut wall to bacteria." The segregation effect seems to offer another explanation for these pure cultures. Question: What happens in the two-species case when the growth curves cross twice?

2 The CSTR versus the PFR

The purpose of this section is to numerically demonstrate the correspondence between the PFR model (with rapid nutrient diffusion and cell motility) and the CSTR models of [6, 10]. We begin with the model of [6].

Here, an invading strain is introduced at the steady state of an already established (resident) strain.

The following assumptions were made in the model:

1. "Resident" and "invader" strains have exactly the same properties.
2. Both strains compete for the same adhesion sites on the gut wall.
3. Both "resident" and "invader" strains compete for the same limiting nutrient.

4. Offspring of adherent microorganisms occupy additional adhesion sites or, when most sites are filled, are shed into the lumen.
5. Adhesion of bacteria is reversible, governed by rate constants for adhesion and dissociation in a mass action type of relation.

Additionally, the intrinsic death rate is assumed to be insignificant.

We now describe the model equations for the PFR under these assumptions. The result is a special case of Model I of [1]; further details can be found there. Consider a long thin tube extending along the x -axis. The reactor occupies the portion of the tube from $x = 0$ to $x = L$. It is fed with growth medium at a constant rate at $x = 0$ due to a constant laminar flow of fluid in the vessel in the direction of increasing x and at velocity v . The external feed contains all nutrients in near optimal amounts except one, denoted S , which is supplied in growth-limiting amounts and at a constant input concentration S^0 . The laminar flow of medium in the tube carries medium, depleted nutrients, organisms, and byproducts out of the reactor at $x = L$. Nutrient is assumed to diffuse throughout with diffusivity d_0 . Free microorganisms are assumed to be capable of random movement, modeled by diffusion coefficients d_i . Wall-attached bacteria are assumed to be immobile. We assume negligible variation of free bacteria and nutrient concentration transverse to the axial direction of the tube.

In addition to the density of nutrient $S(x, t)$, the model accounts for the density of free bacteria, $u_i(x, t)$, and the density of wall-attached bacteria, $w_i(x, t)$. The model takes the form of a system of partial differential equations coupled with a system of ordinary differential equations.

The model equations of two-strain competition in a PFR of radius ρ are given by

$$\begin{aligned}
S_t &= d_0 S_{xx} - v S_x - \gamma_1^{-1} [u_1 + \delta w_1] f_1(S) - \gamma_2^{-1} [u_2 + \delta w_2] f_2(S), \\
(u_i)_t &= d_i (u_i)_{xx} - v (u_i)_x + u_i [f_i(S) - k_i - \alpha_i (1 - W_i)] \\
&\quad + \delta w_i [f_i(S) (1 - G_i(W_i)) + \beta_i], \\
(w_i)_t &= w_i [f_i(S) G_i(W_i) - k_i - \beta_i] + \delta^{-1} \alpha_i u_i (1 - W_i),
\end{aligned} \tag{2.1}$$

for $i = 1, 2$, where $\delta = 2/\rho$, together with the boundary conditions

$$\begin{aligned}
d_0 \frac{\partial S}{\partial x}(0, t) - vS(0, t) &= -vS^0, \\
d_i \frac{\partial u_i}{\partial x}(0, t) - vu_i(0, t) &= 0, \\
\frac{\partial S}{\partial x}(L, t) = \frac{\partial u_i}{\partial x}(L, t) &= 0,
\end{aligned} \tag{2.2}$$

and the initial conditions

$$S(x, 0) = S_0(x) \geq 0, \quad u_i(x, 0) = u_{i0}(x) \geq 0, \quad w_i(x, 0) = w_{i0}(x) \geq 0, \tag{2.3}$$

for $0 \leq x \leq L$. The “resident” strain (respectively, “invader” strain) is referred to as strain one (respectively, strain two).

As in [6], the nutrient uptake functions f_i are assumed to satisfy Monod kinetics:

$$f_i(S) = \frac{m_i S}{a_i + S}.$$

Under assumption 1 we take $m_1 = m_2$ and $a_1 = a_2$. In accordance with assumption 2, the occupation fraction W_i is $W_i = (w_1 + w_2)/w_\infty$, where w_∞ is the maximum bacteria-on-wall density.

The fraction of wall-bound cells finding sites on the wall $G_i(W_i)$, as a function of the occupancy fraction, is assumed to be of the form

$$G_i(W_i) = \frac{1 - W_i}{1 + a - W_i}.$$

In [6] $a = 0.1$, while in [10] $a = 0.01$. We use the latter in all numerical simulations. *This leaves us open to speculation that the choice of $a = 0.01$ plays a role in the correspondence between the PFR and CSTR models. I have rerun the simulation of figure 1 with $a = 0.1$. It seems to make very little difference (see figure 1(b)), and I expect that the same will be the case for the other simulations in the context of [6]. I intend to rerun figures 2 through 4 with $a = 0.1$.*

Free bacteria are attracted to the wall at a rate proportional (with constant α_i) to the product of the free cell density and the fraction of available

wall sites. Finally, we assume that wall-attached bacteria are sloughed off the wall by mechanical forces at a rate proportional (with constant β_i) to their density. Note that we have allowed for the possibility that the rate constants are strain-dependent.

The parameter values used by Freter in figures 1 and 2 of [6] are $m_i = 1.66\text{hr}^{-1}$, $\gamma_i = 0.5$, $a_i = 9.0 \times 10^{-7}\text{g/ml}$, the dilution rate $D = 0.23\text{hr}^{-1}$, $\beta_i = 0.1\text{hr}^{-1}$, $\alpha_i = 1 \times 10^{-7}\text{1/hr g}$, $S^0 = 2.09 \times 10^{-6}\text{g/ml}$, 1g of bacterial mass is assumed to contain 1.8×10^{12} cells, there are 3×10^7 wall sites available for adhesion, and the volume of the growth vessel $V = 1.0\text{ml}$. To establish the correspondence between the two models for large diffusion coefficients, the following modifications are made in the PFR model: $\alpha_i = (1 \times 10^{-7}\text{1/hr g})(3 \times 10^7\text{sites})/[(1.8 \times 10^{12}\text{cells/g})(1 \times 10^{-3}\text{l})] = 1.67 \times 10^{-9}\text{hr}^{-1}$, $v = 0.23\text{hr}^{-1}$ since $D = Q/V$ implies $v = Q/A_c = DL$ and the length of the reactor is assumed to be 1cm, $w_\infty = [(3 \times 10^7\text{sites})/(1.8 \times 10^{12}\text{cells/g})]/(2\pi\rho L\text{cm}^2) = (1.67 \times 10^{-5})/(2\pi\rho L)\text{g/cm}^2$, and $\rho = 0.564$ so that the volume of the reactor is approximately 1ml. To approximate the environment of the CSTR, we take $d_0 = d_i = 3$. Finally, $k_i = 0$, so that intrinsic death rates are considered insignificant.

We obtain the initial conditions as follows. In figure 1 of [6] Freter takes the initial concentration of free residents to be $1.82 \times 10^6\text{cells/ml}$, so that the mass of residents in the lumen is initially $1.0 \times 10^{-6}\text{g}$. This quantity is divided by $\pi\rho^2L\text{ml}$ to obtain the initial condition $u_1(0)$ in the PFR model. Assuming from figure 1 of [6] that \log_{10} of the total number of residents is initially 6.5 yields 3.16×10^6 cells, so that the number of adherent residents is initially $1.34 \times 10^6\text{cells}$. Thus $w_1(0) = (7.4 \times 10^{-7})/(2\pi\rho L)\text{g/cm}^2$ in the plug flow model. (Note that $\log_{10}(1.34 \times 10^6) = 6.13$, in good agreement with figure 1 of [6].) Freter takes the initial number of free invaders to be 1×10^8 , so that $u_2(0) = (5.56 \times 10^{-5})/(\pi\rho^2L)\text{g/ml}$. Since it is assumed that no invaders have occupied sites on the wall at time $t = 0$, $w_2(0) = 0$.

The time series for the PFR model with these parameter values and initial conditions is given in figure 1. The correspondence with figure 1 of [6] is quite remarkable. For high diffusion coefficients, then, the PFR model predicts that a large inoculum of an invader strain with growth, adherence, and dissociation parameters identical to those of the resident strain will be largely washed out. This was observed by Freter and his coworkers both experimentally in [9] and in the CSTR model in [6]. To examine the importance of wall associated growth in the context of figure 1 (and to establish a correspondence with figure 2 of [6]) we take $u_1(0)$ and $u_2(0)$ as above,

$w_1(0) = w_2(0) = 0$, and $\alpha_i = 0$.

The time series for the PFR model is given in figure 2. As in the CSTR model, the invader successfully replaces the resident as the predominant strain in this situation.

As pointed out in [6] the rate of bacterial removal exceeds the maximal growth rate of probably all known bacteria in habitats such as the small intestine. Therefore, only bacteria capable of adhering to the gut wall can colonize this habitat. In contrast, the rate of removal is much slower in the large intestine. Here, colonization is possible without wall growth. (See figure 2.) However, wall growth maintains the stability of the ecosystem by preventing the implantation of invaders, even if they have the same fitness for growth as the residents. (See figure 1.)

The effect of inoculating the PFR of figure 1 with a brief pulse of invaders is depicted in figure 3. Here, $u_2(0) = 0$, $u_2^0 = (5.56 \times 10^{-5})/(\pi\rho^2L)$ g/ml for $0 \leq t \leq 25$, and $u_2^0 = 0$ for $t > 25$. The extent to which competition for wall sites plays a role in figure 1 is illustrated in figure 4, where the invaders and residents are assumed to have strain-specific wall sites available to them. (See Model II in [1].)

Freter [6] indicates that additional computer simulations of the CSTR model point to the exclusion of the less fit bacterial strain when resident and invader are of unequal fitness. The same is true in the PFR model; figure 5 provides an example in which the resident is the less fit bacterial strain. Here, the half-saturation constant of the resident is 1×10^{-6} g/ml while that of the invader is 9×10^{-7} g/ml, all other strain-specific parameters being equal. As can be seen, the invader displaces the resident as the dominant strain after a period of approximately 3000 hours. It should be remembered that the strains compete for both nutrient and adhesion sites in this scenario. When each strain has specific sites for adhesion, the less fit strain may be present on those specific sites and thereby colonize the gut [10]. We next examine this latter situation in the context of the PFR model.

Freter et. al. [10] reformulate the model of [6] to investigate the role of adhesion in the implantation of an invading strain. In this model assumption 1 is relaxed, allowing the resident strain to be a superior competitor on the limiting nutrient. Assumption 2 is also relaxed, so that strains compete for the same limiting nutrient but do not compete for adhesion sites. There are three types of wall sites in the gut where the invader can initially lodge, differentiated by the rate of shedding of attached bacteria. Their model does not consider wall growth of the resident population, since the resident is assumed

to be sufficiently fit to form stable populations and the two populations do not compete for wall sites. In this context the PFR model becomes

$$\begin{aligned}
S_t &= d_0 S_{xx} - v S_x - \gamma_1^{-1} [u_1] f_1(S) - \gamma_2^{-1} [u_2 + \delta w_2] f_2(S), \\
(u_1)_t &= d_1 (u_1)_{xx} - v (u_1)_x + u_1 (f_1(S) - k_1) \\
(u_2)_t &= d_2 (u_2)_{xx} - v (u_2)_x + u_2 (f_2(S) - k_2) \\
&\quad + \delta f_2(S) (w_2^1 (1 - G(W_2^1)) + w_2^2 (1 - G(W_2^2)) + w_2^3 (1 - G(W_2^3)) \\
&\quad - u_2 (\alpha_1 (1 - W_2^1) + \alpha_2 (1 - W_2^2) + \alpha_3 (1 - W_2^3))) \\
&\quad + \delta (\beta_1 w_2^1 + \beta_2 w_2^2 + \beta_3 w_2^3), \\
(w_2^1)_t &= w_2^1 (f_2(S) G(W_2^1) - k_2 - \beta_1) + \delta^{-1} \alpha_1 u_2 (1 - W_2^1), \\
(w_2^2)_t &= w_2^2 (f_2(S) G(W_2^2) - k_2 - \beta_2) + \delta^{-1} \alpha_2 u_2 (1 - W_2^2), \\
(w_2^3)_t &= w_2^3 (f_2(S) G(W_2^3) - k_2 - \beta_3) + \delta^{-1} \alpha_3 u_2 (1 - W_2^3),
\end{aligned} \tag{2.4}$$

together with the boundary conditions (2.2) and initial conditions comparable to (2.3). Here, W_2^j is the invader occupation fraction for sites of type j . It is defined as $W_2^j = w_2^j / w_\infty^j$ where w_∞^j is the wall capacity, specific to the invader, for sites of type j .

The parameter values used by Freter et. al. in figures 10 and 11 of [10] are $m_i = 1.66 \text{hr}^{-1}$, $\gamma_i = 0.5$, $a_1 = 9.1 \times 10^{-7} \text{g/ml}$, $D = 0.23 \text{hr}^{-1}$, $\alpha_i = 1 \times 10^{-7} \text{1/hr g}$, $S^0 = 2.09 \times 10^{-6} \text{g/ml}$, 1g of bacterial mass is assumed to contain 1.8×10^{12} cells, and $V = 1.0 \text{ml}$. The sites available to the invader strain are differentiated as follows: there are 1×10^4 sites with corresponding $\beta_1 = 0.18$, 1×10^3 sites with $\beta_2 = 0.13$, and 1×10^2 sites with $\beta_3 = 0.08$.

To examine the correspondence between the two models for large diffusion coefficients, the following modifications are made in the PFR model: $\alpha_1 = (1 \times 10^{-7} \text{1/hr g})(1 \times 10^4 \text{sites}) / [(1.8 \times 10^{12} \text{cells/g})(1 \times 10^{-3} \text{l})] = 5.56 \times 10^{-11} \text{hr}^{-1}$, $\alpha_2 = 5.56 \times 10^{-12} \text{hr}^{-1}$, and $\alpha_3 = 5.56 \times 10^{-13} \text{hr}^{-1}$. The three invader-specific wall capacities are taken to be $w_\infty^1 = (5.56 \times 10^{-9}) / (2\pi\rho L) \text{g/cm}^2$, $w_\infty^2 = (5.56 \times 10^{-10}) / (2\pi\rho L) \text{g/cm}^2$, and $w_\infty^3 = (5.56 \times 10^{-11}) / (2\pi\rho L) \text{g/cm}^2$. Again, $v = 0.23 \text{hr}^{-1}$, $\rho = 0.564$, $k_1 = k_2 = 0$, and $d_0 = d_1 = d_2 = 3$. For the initial conditions, Freter et. al. [10] take the initial concentration of free residents to be 1×10^6 cells/ml and the initial concentration of free invaders to be 1×10^8 cells/ml; the corresponding values for the plug flow reactor are obtained as in the previous case.

The simulations run in the context of [10] are shown in figure 6. In figure 6(a) the parameter values and initial conditions are as in figure 10

of [10], so that $a_2 = 1.9 \times 10^{-6}$ g/ml. The same is true of figure 6(b) and figure 11 of [10], so that $a_2 = 1.1 \times 10^{-6}$ g/ml. Note that the time series in figure 6(b) closely resembles that of figure 11 of [10], while figure 6(a) depicts a situation lying between figures 10 and 11 of [10]. When the disparity between the resident and invader is increased by taking $a_2 = 3.2 \times 10^{-6}$ g/ml, as in figure 6(c), we obtain a time series more closely resembling figure 10 of [10]. Thus, as in the CSTR model [10], stable populations of two bacterial strains that compete in the gut for the same limiting nutrient can coexist if the less fit strain has specific adhesion sites available. (See figures 6(a) and (b).) If the growth rate of the less fit strain is lowered, this strain will be unable to colonize the less sheltered wall areas, but may still persist in those areas where the slough-off rate is slower. (See figure 6(c).) Finally we note that the invader washed out completely when a_2 was increased further still. This is again consistent with the results of Freter et. al. for the CSTR model [10].

3 The PFR revisited

The results of the previous section were obtained for large diffusion coefficients. In this section we take advantage of the structure of the PFR model and frame the numerics in a biologically reasonable context. The basic dimensions of the reactor are chosen in accordance with data on the large intestine provided by Mitsuoka [16]. Thus, the length $L = 150$ cm and the radius $\rho = 2.5$ cm. The velocity of the medium is varied to approximate transit times between 12 and 48 hours [17]. The random motility coefficients are taken to be $d_i = 0.2$ cm²/hr (see [21]), while the nutrient is assumed to diffuse with diffusivity $d_0 = 0.0002$ cm²/hr (see [3]). The nutrient uptake functions again satisfy Monod kinetics, and the fraction of daughter cells of wall-bound bacteria finding sites on the wall $G_i(W_i)$ is again taken to coincide with that of Freter et. al. [10]. The parameters describing growth, adhesion, and slough-off will be described below. They will be chosen so that direct comparisons with the simulations of the previous section can be made.

4 Nomenclature

$u_i(x, t)$	Bacteria-in-solution density of population u_i
d_i	Diffusion coefficient for population u_i
$w_i(x, t)$	Bacteria-on-wall density of population w_i
w_∞	Maximum bacteria-on-wall density
$w_2^j(x, t)$	Bacteria-on-wall density of population w_2 for sites of type j
w_∞^j	Maximum bacteria-on-wall density, specific to the invader, for sites of type j
$W_i(x, t)$	Strain-specific occupation fraction.
$W_2^j(x, t)$	Invader occupation fraction for sites of type j , $W_2^j = w_2^j/w_\infty^j$
G_i	Fraction of offspring of population w_i which find sites on the wall.
$S(x, t)$	Nutrient density
d_0	Diffusion coefficient for resource S
S^0	Input concentration of resource S
$f_{u_i}(S), f_{w_i}(S)$	Resource dependent growth rate of population u_i, w_i per unit of population u_i, w_i
γ_i	Growth yield constant for strain i on resource S
k_{u_i}, k_{w_i}	Intrinsic death rate of population u_i, w_i
α_i	Rate coefficient of attachment for population u_i
β_i	Rate coefficient of detachment for population w_i
L	Length of the reactor
ρ	Radius of the reactor
v	Volumetric flow rate

References

- [1] Ballyk, M., Smith, H. (1998) A Flow reactor with Wall Growth, accepted ...
- [2] Ballyk, M., Smith, H. (1998) A Model of Microbial Growth in a Flow reactor with Wall Growth, accepted ...
- [3] Berg, H.C. (1983) Random Walks in Biology, Princeton University Press, Princeton, N.J.

- [4] Drassar, B.S., Hill, M.J. (1974) *Human Intestinal Flora*, Academic Press Inc. Ltd., London.
- [5] Finegold, S.M., Sutter, V.L., Mathisen, G.B. (1983) Normal indigenous intestinal flora, in *Human Intestinal Microflora in Health and Disease*, D. Hentges (ed.), Academic Press, New York.
- [6] Freter, R. (1983) Mechanisms that control the microflora in the large intestine, in *Human Intestinal Microflora in Health and Disease*, D. Hentges (ed.), Academic Press, New York.
- [7] Freter, R. (1984) Interdependence of mechanisms that control bacterial colonization of the large intestine, *Microecology and Therapy* 14, 89-96.
- [8] Freter, R., Stauffer, E., Cleven, D., Holdeman, L.V., Moore, W.E.C. (1983) Continuous-flow cultures as in vitro models of the ecology of large intestinal flora, *Infect. Immun.* 39, 666-675.
- [9] Freter, R., Brickner, H., Botney, M., Cleven, D. Aranki, A. (1983) Mechanisms that control bacterial populations in continuous-flow culture models of mouse large intestinal flora, *Infect. Immun.* 39, 676-685.
- [10] Freter, R., Brickner, H., Fekete, J., Vickerman, M.M., Carley, K.E. (1983) Survival and implantation of *Escheridia coli* in the intestinal tract, *Infect. Immun.* 39, 686-703.
- [11] Freter, R., Brickner, H., Temme, S.J. (1986) An understanding of colonization resistance of the mammalian large intestine requires mathematical analysis, *Microecology and Therapy* 16, 147-155.
- [12] Hume, I.D. (1997) Fermentation in the hindgut of mammals, in *Gastrointestinal Microbiology*, R.I. Mackie, B.A. White (eds.), Chapman and Hall Microbiology Series, New York.
- [13] Lee, A. (1985) Neglected niches: The microbial ecology of the gastrointestinal tract, in *Advances in Microbial Ecology*, Plenum Press, New York.
- [14] Macfarlane, G.T., Macfarlane, S. (1997) Human colonic microbiota: Ecology, physiology, and metabolic potential, *Proc. Nutr. Soc.* 52:367-373.

- [15] Macfarlane, G.T., Macfarlane, S., Gibson, G.R. (1998) Validation of a three-stage compound continuous culture system for investigating the effect of retention time on the ecology and metabolism of bacteria in the human colon, *Microbial Ecology* 35:180-187.
- [16] Mitsuoka, T. (1978) *Intestinal Bacteria and Health: An Introductory Narrative*, Harcourt Brace Jovanovich Japan, Tokyo.
- [17] Patton, H.D., Fuchs, A.F., Hille, B., Scher, A.M., Steiner, R., *Textbook of Physiology*, Vol 2, 21st edition, W.B. Saunders Co., Philadelphia, 1989.
- [18] Penry, D. and Jumars, P., Modeling animal guts as chemical reactors, *American Naturalist* 129 (1987) 69-96.
- [19] Rolfe, R.D. (1997) Colonization Resistance, in *Gastrointestinal Microbiology*, R.I. Mackie, B.A. White, R.E. Isaacson (eds.), Chapman and Hall Microbiology Series, New York.
- [20] Savage, D.C. (1985) Effects on host animals of bacteria adhering to epithelial surfaces, in *Bacterial Adhesion*, D.C. Savage, M.M. Fletcher (eds.), Plenum Press, New York.
- [21] Segel, L.A. (1984) *Modeling Dynamic Phenomena in Molecular and Cellular Biology*, Cambridge University Press, N.Y.
- [22] Van der Waaij, D., Berghuis-de vries, J.M., Lekkerkerk-van der Wees, J.E.C. (1971) Colonization resistance of the digestive tract in conventional and antibiotic-treated mice, *J. Hyg.* 69, 405-413.

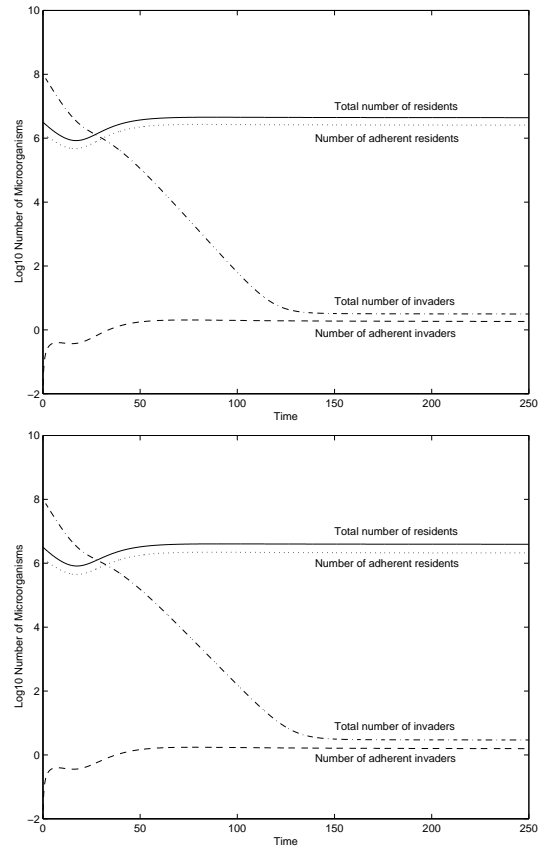


Figure 1: Time series for flow reactor in which an invader strain competes with a resident strain for the same adhesion sites and the same limiting nutrient. (a) $a = 0.01$, (b) $a = 0.1$.

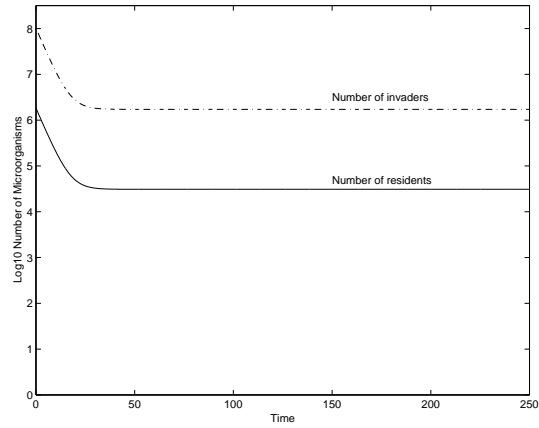


Figure 2: Time series for the same interactions shown in figure 1 except that there is no wall growth.

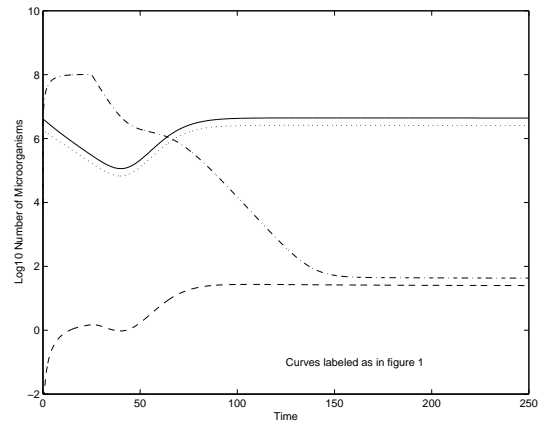


Figure 3: Time series for the same interactions shown in figure 1 except that the reactor is innoculated with the invading strain via a brief initial pulse from the feed.

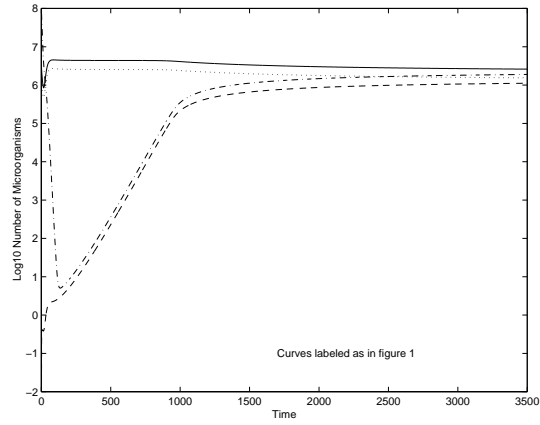


Figure 4: Time series for the same interactions shown in figure 1 except that there is no competition for wall sites. The wall is made up of strain-specific sites.

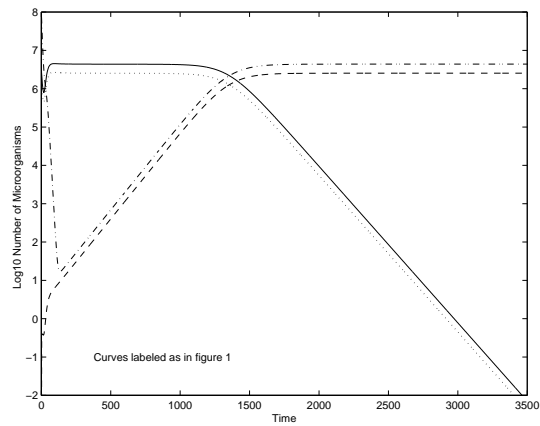


Figure 5: Time series for the same interactions shown in figure 1 except that the resident and invading strains are of unequal fitness. The half-saturation constant for the resident is 1×10^{-6} g/ml while that of the invader is 9×10^{-7} g/ml, so that the resident is the less fit bacterial strain.

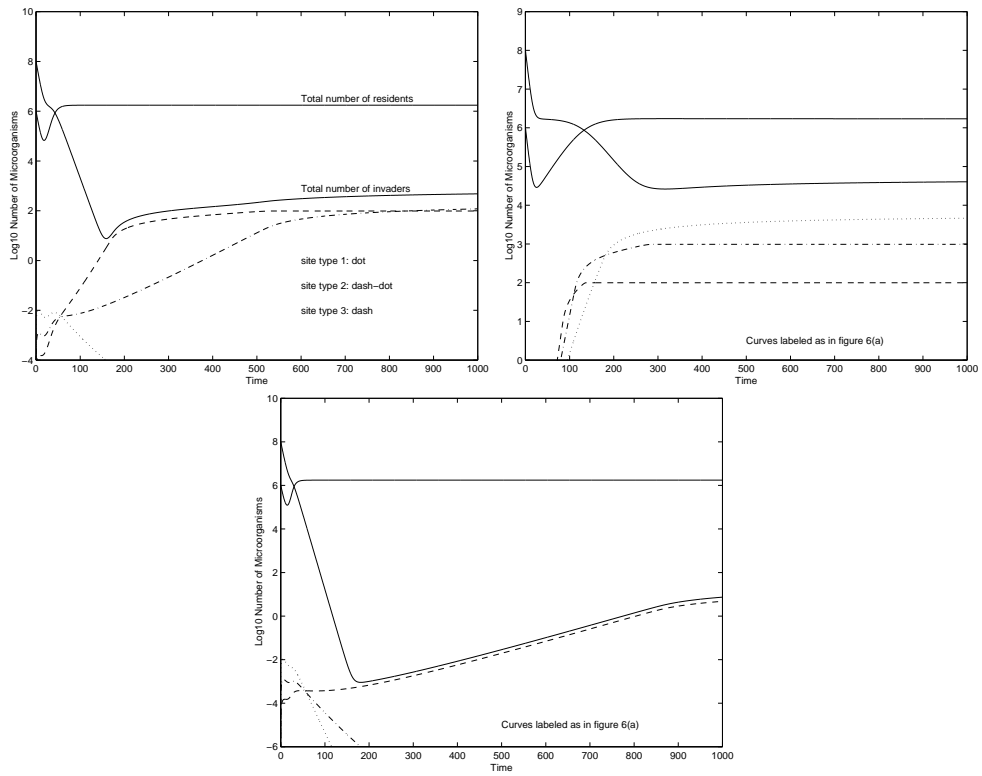


Figure 6: Time series for the plug flow reactor in which is made up of strain-specific sites. The sites specific to the invader are further differentiated by the rates of adhesion and detachment. In figure 6(a), $a_i = 1.9 \times 10^{-3}$. In figure 6(b), $a_i = 1.1 \times 10^{-3}$. In figure 6(c), $a_i = 3.2 \times 10^{-3}$.

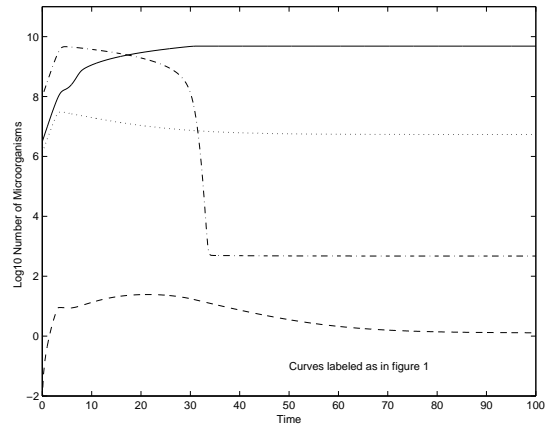


Figure 7: Time series for the same interactions as in figure 1 with realistic parameter values as described in section 3.

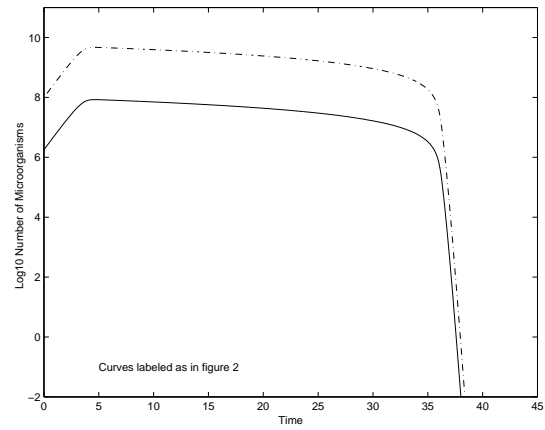


Figure 8: Time series for the same interactions as in figure 2 with realistic parameter values.

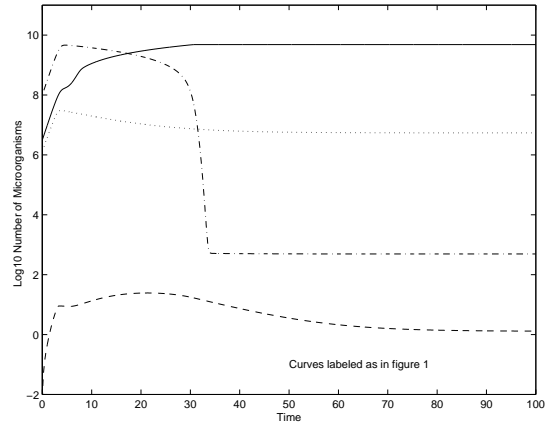


Figure 9: Time series for the same interactions shown in figure 1 with realistic parameter values. Here the invading strain is more motile than the resident: $d_1 = 0.02$ and $d_2 = 0.2$.

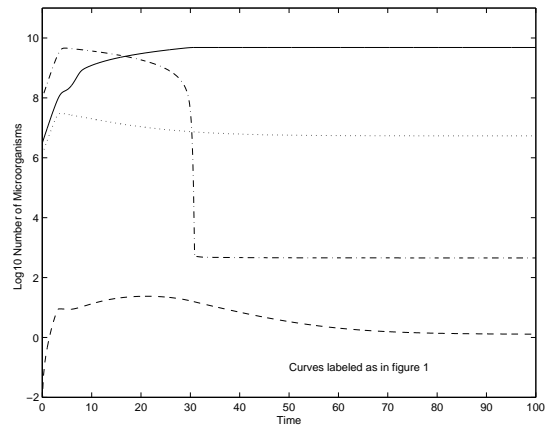


Figure 10: Time series for the same interactions as in figure 1 with realistic parameter values. Here the resident strain is more motile than the invader: $d_1 = 0.2$ and $d_2 = 0.02$.

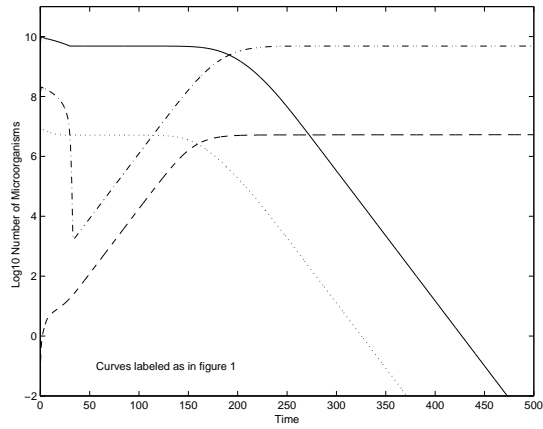


Figure 11: Time series for the same interactions shown in figure 1 with realistic parameter values. Here the resident and invader are equally motile. The invader is assumed to attach more readily and adhere more avidly than the resident: $\beta_1 = 0.2$ and $\alpha_1 = 1.67 \times 10^{-9}$, while $\beta_2 = 0.1$ and $\alpha_1 = 3.34 \times 10^{-9}$.

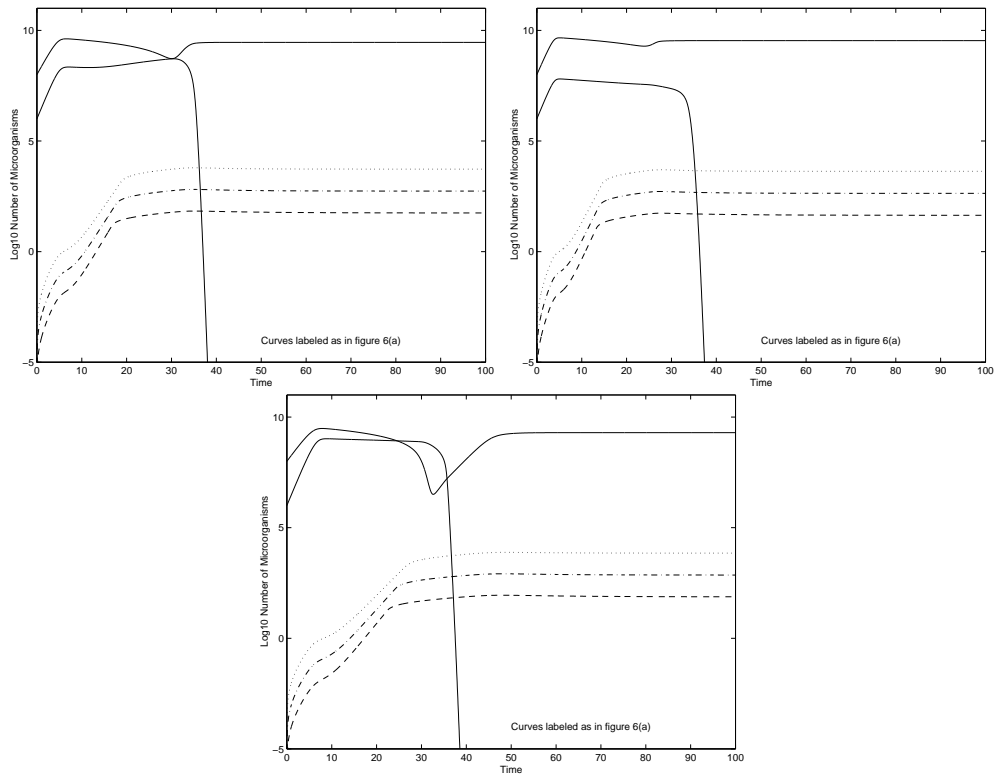


Figure 12: Time series for the same interactions shown in figure 6 with realistic parameter values. (*The resident is the one dying out.*)

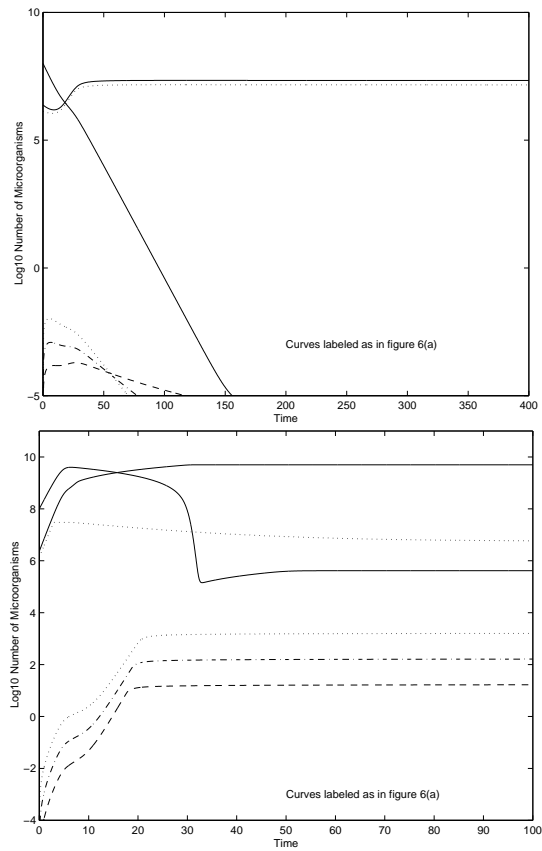


Figure 13: Time series for the same interactions shown in figure 6(a) and figure 12(a). Here, wall growth is incorporated into the model for the resident strain.